MEMORANDUM
RM-5598-RC
DECEMBER 1969

A SIMULATION STUDY OF COINCIDENCE DETECTION IN THE DENDRITES OF A SINGLE NERVE CELL

R. J. MacGregor

The RAND Corporation
SANTA MONICA • CALIFORNIA

MEMORANDUM
RM-5598-RC
DECEMBER 1969

A SIMULATION STUDY OF COINCIDENCE DETECTION IN THE DENDRITES OF A SINGLE NERVE CELL

R. J. MacGregor

The RAND Corporation

This study is presented as a competent treatment of the subject, worthy of publication. The Rand Corporation vouches for the quality of the research, without necessarily endorsing the opinions and conclusions of the authors.

Published by The RAND Corporation

PREFACE

This Memorandum represents a portion of a total Rand program in the biological sciences, various parts of which have been sponsored by The Rand Corporation, the Advanced Research Projects Agency, and the United States Air Force. This program includes work on the fluid mechanics of blood flow, image enhancement, and stroke detection, as well as the present research, which is concerned with the functional organization of the nervous system.

Several factors have motivated the present study. First, the questions of coincidence sensitivity of nerve cells and its functional significance have confronted the author in his studies of spatial and temporal interaction in color vision. Second, a Rand colleague, D. H. Perkel, has pointed out to the author the possible applicability of the proposed mechanism to the Purkinje cells of the cerebellum. The latter provide an extremely propitious point of focus for the proposed mechanism both because there exists extensive histological and neuro-electrical data from the cerebellar network and because one has anatomical and functional reasons to suspect that the Purkinje cells might indeed utilize sharp coincidence sensitivity. Third, the author's previous work concerning mechanisms of interactions in dendrites has provided simulation programs whereby the proposed mechanism might be readily examined. Finally, and perhaps most importantly, the concept is of considerable import to the general field of information processing in neural networks.

Previous Rand publications on related topics include RM-4877-ARPA, A Digital-Computer Model of Spike Elicitation by Postsynaptic Potentials in Single Nerve Cells, and P-3672, Input-Output Relations for Axo-Somatic Activation in a Neuron Model.

SUMMARY

This Memorandum presents the results of simulations which indicate the ability of a typical nerve cell to discriminate between coincident pulses as compared with two pulses a short time-interval apart. The simulations are performed with a model for neuroelectric coding processes in a single cell, which includes a representation of dendritic geometry. For this model: (a) the probability, p, that an output spike will be associated in time with a coupled pair of input pulses originating at dendritic synapses is greater when the time interval between the pulses is 0 than when it is 2 msec; (b) both the actual values of probabilities and their differences, $p(\Delta T = 0) - p(\Delta T = 2)$, are generally larger for smooth than for irregular background activity, and both the probabilities and their differences tend to display maxima at intermediate levels of background activity; and (c) the difference $p(\Delta T = 0) - p(\Delta T = 2)$ is greater the closer together the two synapses.

ACKNOWLEDGMENTS

The author expresses appreciation to Professor John W. Moore (of Duke University) for helpful commentary concerning this work; to Donald H. Perkel for providing computer programs to help analyze the data; and to Jeannine Lamar for assistance with the computations.

CONTENTS

PREFACE iii

SUMMARY v

Section
I. INTRODUCTION. 1

II. METHODS 3

III. RESULTS 10

IV. DISCUSSION AND CONCLUSIONS. 32

REFERENCES. 39

I. INTRODUCTION

This Memorandum deals with the ability of single nerve cells to detect the coincidence of two input pulses. In particular we are concerned with a nerve cell's ability to discriminate between input patterns which contain two simultaneous pulses and those which contain two pulses separated by a small interval of time.

This is clearly a crucial question as regards the function of neural subsystems. Many (probably most) nerve cells are activated by an ongoing barrage of all-or-none spike potentials in the collection of fibers which impinge upon them. The temporal structure of the input pattern (in a given geometry) is its most salient distinguishable characteristic. If a cell is able to respond selectively to input patterns, it is most likely that the interpulse interval pattern of the input determines the selection to be made.

A bothersome observation in this regard is that post-synaptic potentials (PSPs) generally extend over a rather lengthy time interval (perhaps 5 to 30 times as long as the input permeability change which initiates them). Thus, the resultant potential obtained by pure addition of two PSPs whose starting times are separated by, say, 2 msec exhibits a peak value and general shape which are very little different from those obtained by adding two simultaneous PSPs. Moreover, when PSPs are propagated along passive membrane they are very markedly broadened and flattened.

The vast majority of input synapses occur on the dendrites of nerve cells, and probably the majority of nerve cells exhibit passive membrane in their dendrites. Thus, a significantly large fraction of graded responses in nerve cells as seen at the soma of the cells exhibits a generally broad and flat character, with rather slow rising and falling phases. If one adds (on paper) two identical graded responses of such a character, the difference between the resultants obtained for two simultaneous responses on the one hand, and for two responses a short time apart on the other, appears very small indeed.

It is not at all clear, then, that the "standard" or "canonical" nerve cell (which generates at its soma output spike trains on the

basis of graded synaptic responses), operating according to the conventional notions of spatial and temporal summation, can discriminate small differences in interpulse intervals of input patterns. Such a limitation would greatly reduce the potential coding repertoire of the cell as regards the vast majority of its input fibers. This, in turn, would severely limit the role of the cell in the subsystem of which it is part.

Since this conclusion has bothered us, we have performed simulation studies to investigate the ability of the "standard nerve cell" to detect the coincidence of input pulses. We have explored the ways in which responses obtained for two simultaneous pulses differ from those obtained for two pulses one and two msec apart. In the present study we are primarily concerned with the coincidence of pulses at two neighboring synapses in dendrites.

To anticipate, the simulation model discussed herein has led us to the following conclusions:

- output spikes are more likely to occur for two coincident input pulses than for two pulses separated by 2 msec;
- output spikes are more likely to be sharply locked in time to an input event when the input event consists of two coincident pulses than when it consists of two pulses 2 msec apart;
- the foregoing observations hold for input events which result in very broad PSPs as observed at the "trigger" section (intended to represent responses from synapses in dendrites about 1¼ length constants from the soma);
- finally, the sensitivity to coincidence of input pulses is greater for synapses whose currents interact than for synapses whose currents do not interact, and as a corollary, is greater the closer together the two synapses.

II. METHODS*

Our simulations are intended to represent the neuroelectric coding processes of the "standard nerve cell". For us, the "standard nerve cell" is defined as follows:

The input portion of the cell consists of passive membrane (and consequently graded potentials) in the dendrites and soma, and all-or-none spike potentials are triggered at the axon hillock and propagated without decrement along the axon of the cell which serves as the output channel; PSPs are induced in the passive regions by changes in the permeability of subsynaptic membrane according to activity in the presynaptic fiber; PSPs are propagated along the passive membrane to the triggering section, where a time series of output spikes is generated according to a threshold rule which operates on the resultant of the graded potentials from all input synapses. There are essentially two sources of nonlinearity in this concept: one source is the possibility of interaction between inputs at the synapses (since the input driving force is a permeability change -- not a potential, per se -- input pulse amplitudes are diminished by prior potential); the second is the process of spike generation by the threshold rule.

Our simulations have been performed on a digital computer using a computational model designed to represent the behavior of the standard nerve cell (as defined above). The model can accommodate an arbitrary number of synapses in any desired spatial arrangement. This is accomplished by reading in a matrix whose elements specify the distances from each synapse to all the other synapses and to the soma. The input pulse rates and the relative time phase of activity can be specified independently for all the synapses. Each input time so determined corresponds to the initiation of a simulated PSP which propagates and decays according to

---

*The background for the present work and methods is described in References 1 to 5.

$$PSP = A \frac{\exp\left[\frac{-(|x - x^*| + 1)^2}{4(t - t^*)} - (t - t^*)\right]}{\sqrt{(t - t^*)}} \qquad (1)$$

Here x^* is the location of the synapse and t^* is the time of the particular input event. The influence of every PSP is evaluated at the soma and at every other synapse (at times when the latter are activated) according to the values assigned to $x - x^*$. These in turn have been specified according to the input matrix. Figure 1 shows the shape of PSPs determined by this function.

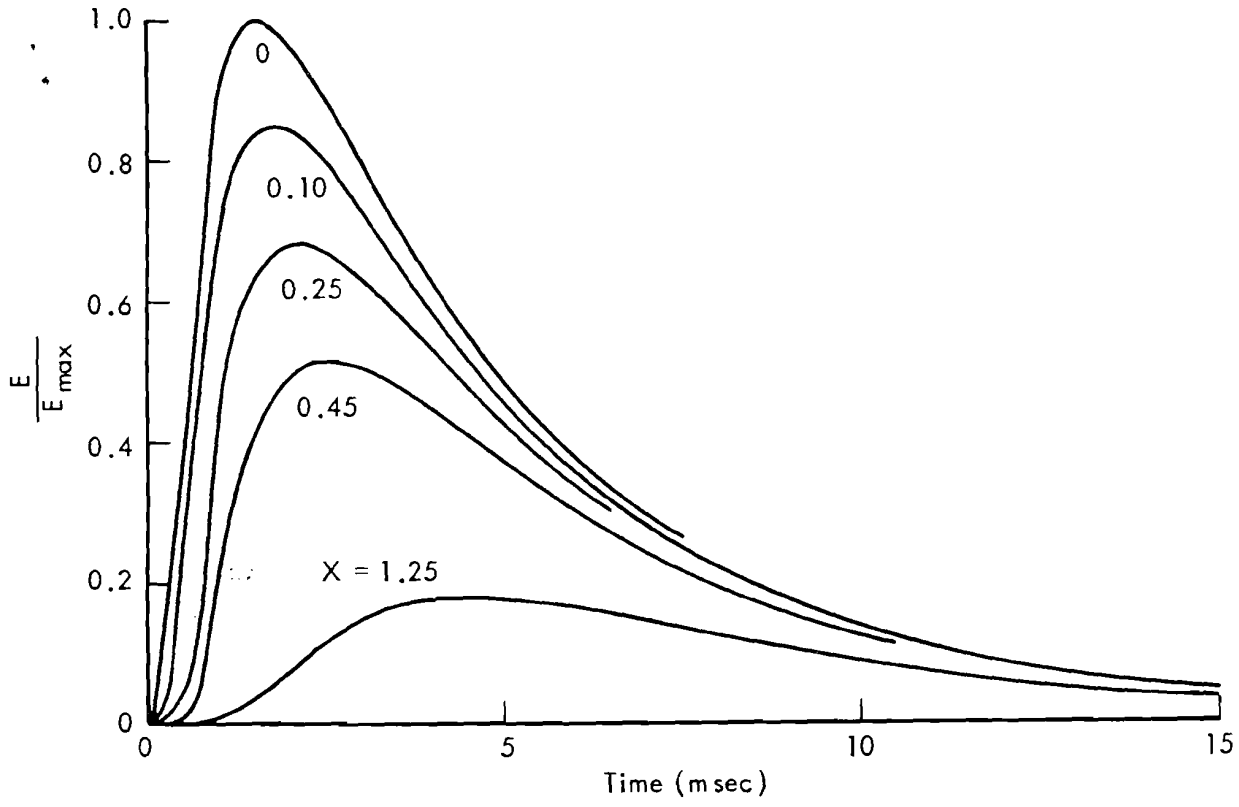

Fig. 1 -- Representation of PSPs in the model.

PSPs interact in our model according to the following rule:

$$A = \begin{cases} A_o & , E_o < 15 \text{ mv} \\ A_o \left(1 - \dfrac{E_o - 15}{55}\right), & E_o > 15 \text{ mv} \end{cases} \qquad (2)$$

A is the amplitude of the PSPs at a particular synapse; A_o is a specified control pulse amplitude; and E_o is the potential at the synapse in question at the time it is activated.*

PSPs from all sources are summed by a routine in the model which is intended to represent the processes at the axon hillock. A threshold rule is used to determine whether an output spike has been generated. A control threshold value is read into the program so that one may observe entirely graded activity simply by setting this value sufficiently high. If a spike is generated at a given time, that time is recorded and refractoriness follows. Refractoriness is simulated by allowing no spikes in a certain predetermined interval (absolute refractoriness), and by initiating negative after-potentials to be summed with ongoing graded input potentials and temporarily raising the threshold value (relative refractoriness). Also, the model simulates the propagation of output spikes back into dendrites according to

$$E(x,t) = \frac{A}{2}\left[e^{x}\left\{\operatorname{erfc}\left[(t)^{\frac{1}{2}} + \frac{x}{2(t)^{\frac{1}{2}}}\right] - \operatorname{erfc}\left[(t-t^*)^{\frac{1}{2}} + \frac{x}{2(t-t^*)^{\frac{1}{2}}}\right]\right\}\right.$$
$$\left. - e^{-x}\left\{\operatorname{erfc}\left[(t)^{\frac{1}{2}} - \frac{x}{2(t)^{\frac{1}{2}}}\right] - \operatorname{erfc}\left[(t-t^*)^{\frac{1}{2}} - \frac{x}{2(t-t^*)^{\frac{1}{2}}}\right]\right\}\right] \qquad (3)$$

This potential is then added to subsequent evaluations of E_o in Eq. (2) and thereby influences the amplitude of subsequent input PSPs.

---

*The present paper deals only with excitatory input; the general model can treat inhibitory input as well by changing the numbers 15 and 55 in Eq. (2) (which correspond to an equilibrium potential of 70 mv) and using negative values of A_o.

Finally, the times of the output spikes are recorded on punched cards as output from the model. These, together with similar time series representing the temporal structure of the input, are analyzed by a separate program designed for this purpose by D. H. Perkel.[7]

Most of the simulations reported in the present paper deal with the dendritic geometry illustrated in Fig. 2.

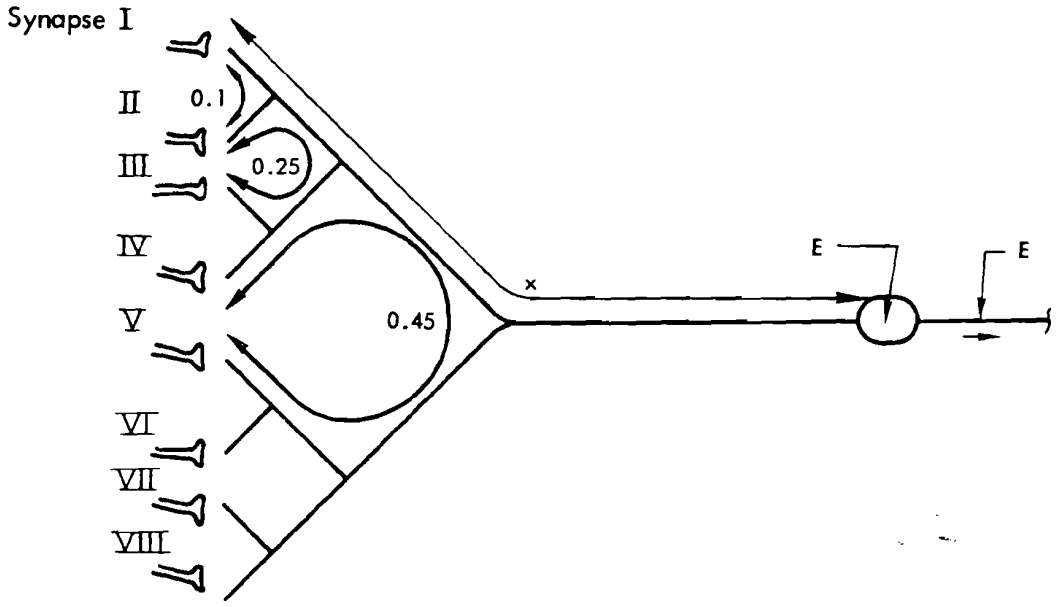

Fig. 2 -- Pattern of branching dendrites used in simulations.

The branching pattern shown in Fig. 2 is symmetric: each synapse is 0.1 length constant away from one other synapse, 0.25 length constant from two other synapses, and 0.45 length constant from four other synapses; all synapses are 1.25 length constants from the soma.

The temporal structure of the input is determined by specifying two parameters for each synapse: the input rate (w) and the time of the first pulse (t_o). We will be concerned with four input patterns as defined in Table 1. (The values given in Table 1 correspond to the spatial location of synapses shown in Fig. 2.)

Table 1

PARAMETERS w AND t_o FOR FOUR INPUT PATTERNS

	Random		ΔT = 2		ΔT = 1		ΔT = 0	
Synapse	t_o	w	t_o	w	t_o	w	t_o	w
I	19.27	47.35	13.14	58.525	13.14	58.525	13.14	58.525
III	7.01	69.70	15.14	58.525	14.14	58.525	13.14	58.525
II	13.49	63.20						
IV	7.21	47.00						
V	2.96	49.20						
VI	2.32	31.15						
VII	.10	50.60						
VIII	12.53	33.20						

The values of t_o and w are the same in all cases for synapses IV - VIII.

All four patterns have a mean rate of 391.2 pulses per second. The first pattern, hereafter referred to as "random", was determined by a random-number generator. Each of the other three patterns contains a repeatedly presented confluence of two input pulses. In particular, the input pulses in synapses I and III are systematically coupled in each of these cases. The cases labeled ΔT = 0, 1, and 2 correspond respectively to the situations where pulses in synapse I and III are coincident, are separated by 1 msec, and by 2 msec. The random case serves as a referrent from which we may gauge for example, the relative influence of a single PSP under these conditions. We are interested in how the responses for the cases labeled ΔT = 0, 1, and 2 differ from the random case, and more importantly, how they differ from each other. One may view these cases as presenting a specified coupled pair of pulses to the cell against a background activity of $391.2 - (2 \times 58.525) = 275$ pulses per second. The coupled pulses originate in synapses 0.25 length constants apart (synapses I and III).

The temporal structures of the four input patterns as wholes (that is, pulses from all eight synapses considered together as a single input pattern) are shown in Fig. 3.

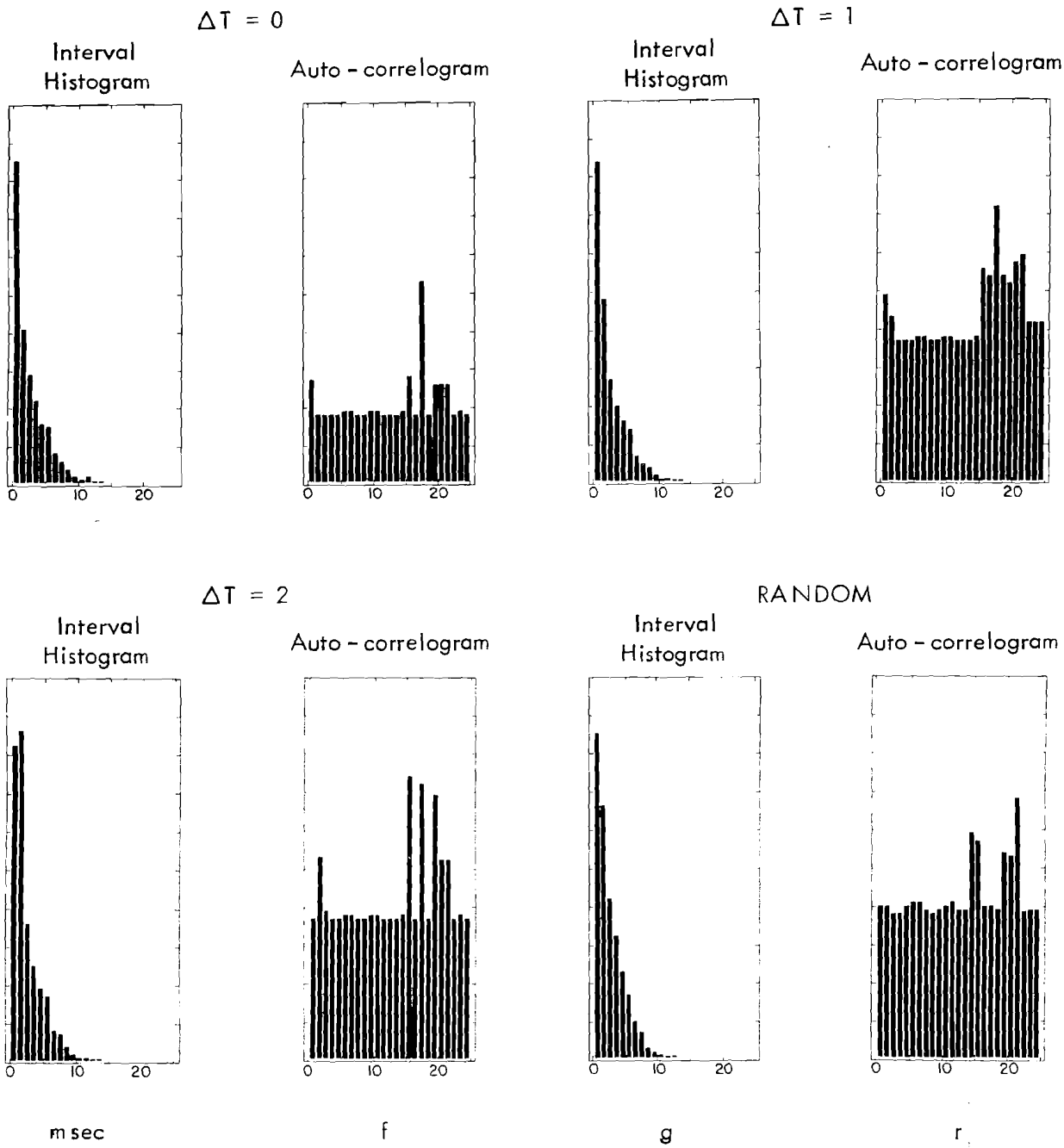

Fig. 3 -- Temporal structure of input patterns.

We have performed simulations of two kinds with these input patterns. In the first kind, hereafter called "interacting", the individual PSPs interact with one another according to Eq. (2) and the geometry shown in Fig. 2. For this case, all the individual PSPs have a control amplitude of 25 mv as observed at the synapses. For the second kind, hereafter referred to as "noninteracting", the distances between the synapses have been set at a very high value so that they do not interact. All the synapses are still equidistant from the soma (1.25 length constants in our approximation). In this case, the individual PSP amplitudes are 19.1 mv as observed at the synapses. (This value was chosen so that the output frequencies for the two kinds of input would have roughly the same values.)

Thus, eight input patterns are considered. We have obtained a sample of graded response to each of these eight patterns by setting the threshold in the model at a sufficiently high value. Also, for each of the eight input patterns we have obtained output spike trains at each of six threshold values: 4, 6, 8, 9.5, 9.9, and 10 mv. Each such spike train results from a six-second sample of activity; each of the cases containing coupled pairs, then, represents $6 \times 58.25 \approx 350$ presentations of the pair. It is easy to see that one may interpret our results in a probabilistic sense, wherein each event of interest has been presented against a large number of random samples of the refractory state of the cell, the current value of the graded generator potential, the recent history of output spikes, and potentials at each of the two synapses. This indeed is the way we interpret our results.

Altogether, then, 48 output spike trains are considered in this primary example.

Also, we have performed one set of simulations where the coupled pulses occur in two synapses 0.1 length constant apart. Finally, a set of simulations has been performed to indicate how the magnitude of the background activity influences coincidence sensitivity.

III. RESULTS

GRADED RESPONSES

Figure 4 shows graded responses in the model for 100-msec samples from each of the eight input patterns. The arrows show the times when the first of the two coupled pulses are initiated. Figure 4 shows that the peak amplitudes in the graded response are larger for coincident pulses than for $\Delta T = 1$ or $\Delta T = 2$, and are larger for our interacting synapses than for our noninteracting synapses. (Since the threshold has been set arbitrarily high in these samples, the refractory mechanisms of the model are not shown in Fig. 4.)

The responses shown in Fig. 4 are samples of the generator potential from which output spikes are derived according to a threshold rule. In the following section we will describe properties of the output spike trains generated in our model by the patterns shown in Fig. 4 for six different control threshold values: 10, 9.9, 9.5, 8, 6, and 4 mv.

OUTPUT SPIKE TRAINS

We wish to show here that (with a minor exception to be discussed below) the coupled pair of coincident input pulses is more likely to be associated with an output spike than is the pair $\Delta T = 2$, and that the difference between responses for $\Delta T = 0$ and $\Delta T = 2$ is greater than suggested by pure summation of PSPs and is greater for the interacting case than for the noninteracting case. These points will be illustrated for the results obtained when the threshold was 10 mv; then results for all 48 cases will be presented.

THRESHOLD = 10 mv

Figure 5 shows the interspike interval and autocorrelation histograms for the input and corresponding output spike trains, and their cross-correlation histograms for the interacting case with a control threshold of 10 mv.

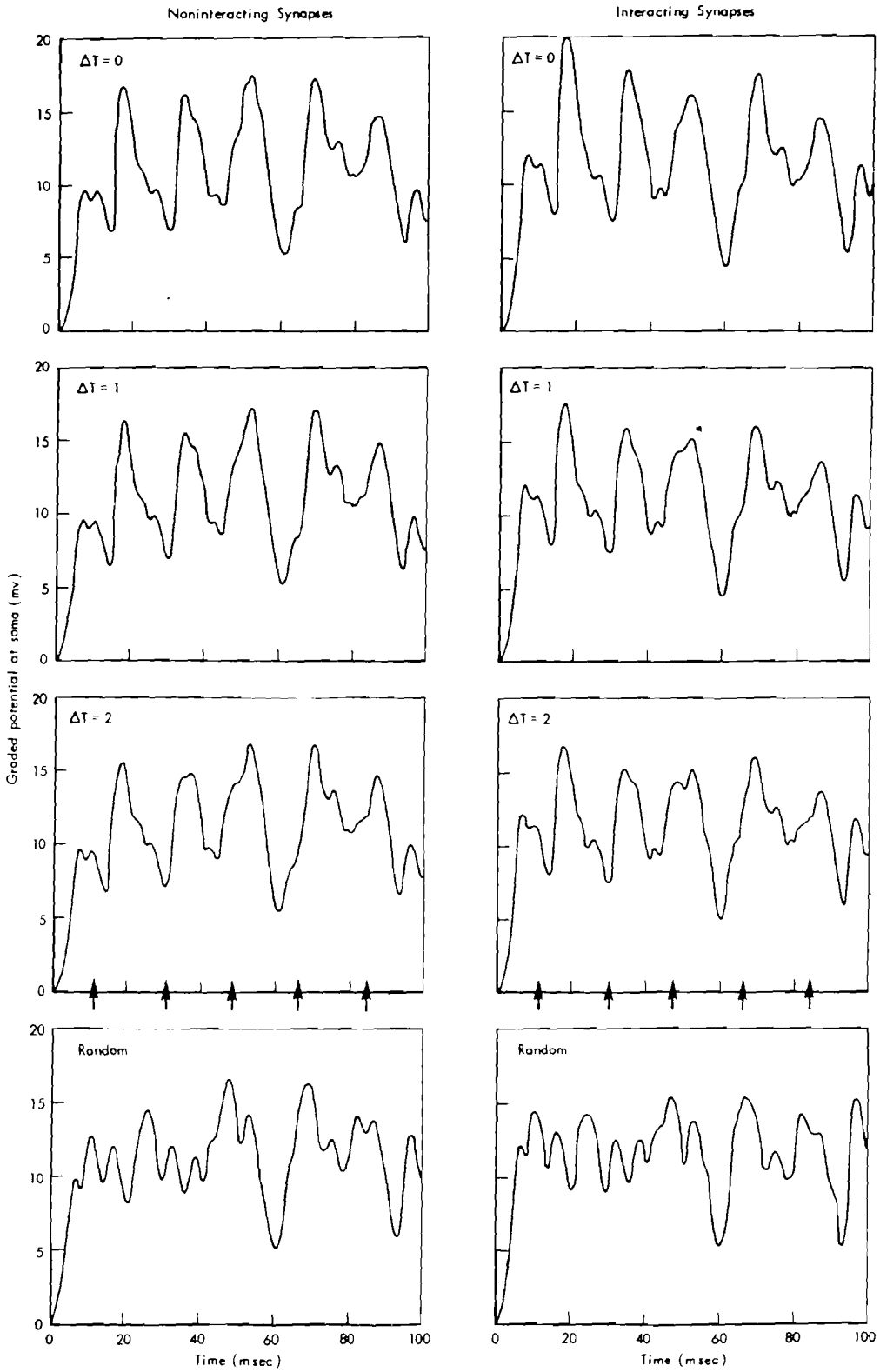

Fig. 4 -- Graded responses for eight basic input patterns.

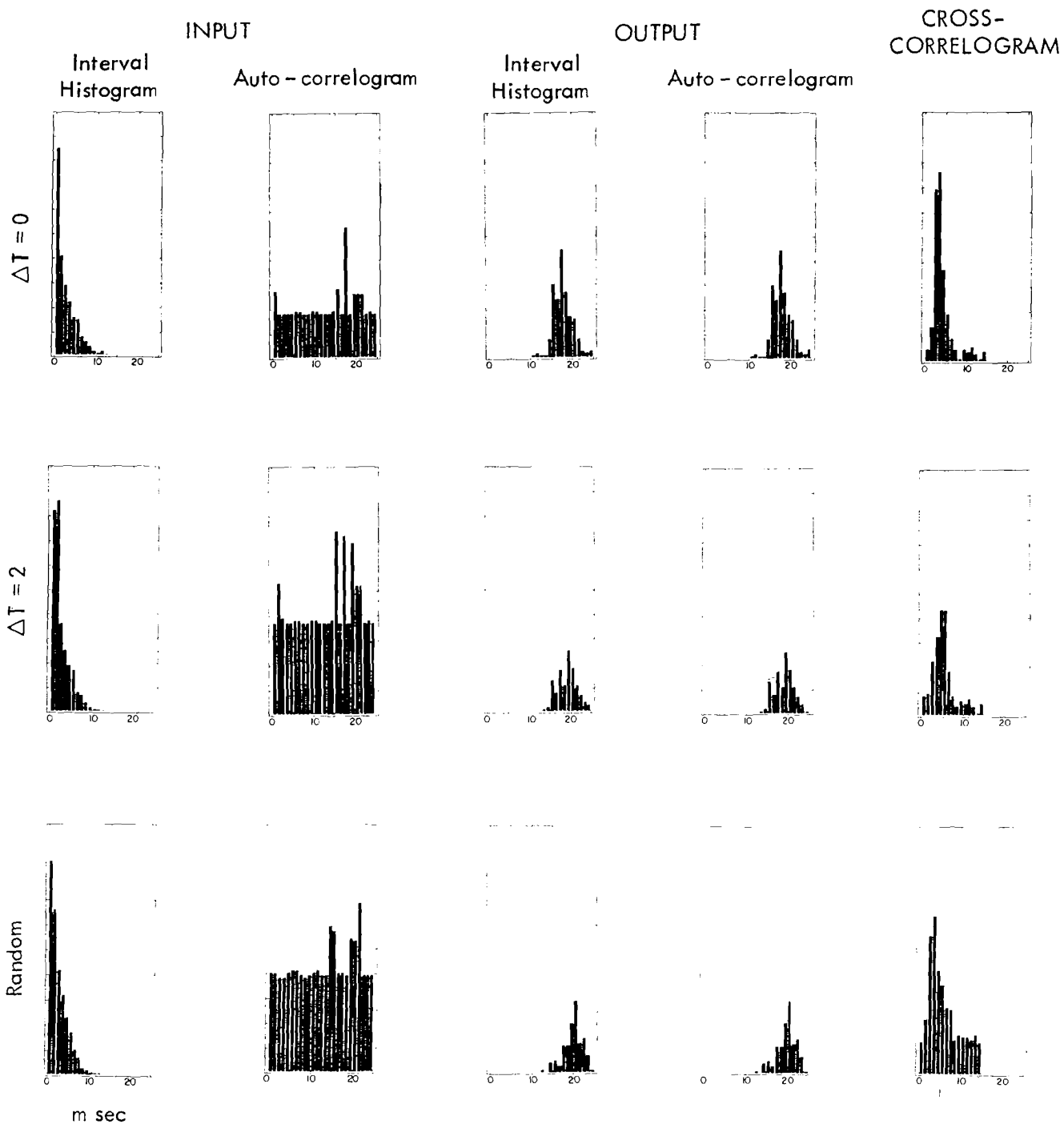

Fig. 5 -- Temporal structure of input-output transfer for interacting synapses.

The cross-correlation histogram (when appropriately normalized) may be interpreted as the probability that an output spike will occur in a given time bin, given that the input event occurred at time t = 0. For the cases $\Delta T = 0$, 1, and 2 in our computations the input event is the initiation of the first input pulse in the coupled pair. Thus for these cases our cross-correlation histograms may be interpreted as post-stimulus histograms wherein the coupled input pulses are the stimuli. In the random case, all the input pulses were tabulated for the cross-correlation histograms.

Figure 6 shows our cross-correlation probability curves for both the interacting and noninteracting cases when the control threshold was 10 mv. The essential conclusions of this paper are illustrated in Fig. 6, We note first that the probability curves for $\Delta T = 0$ are higher than for $\Delta T = 2$, and second, that the difference between the curves

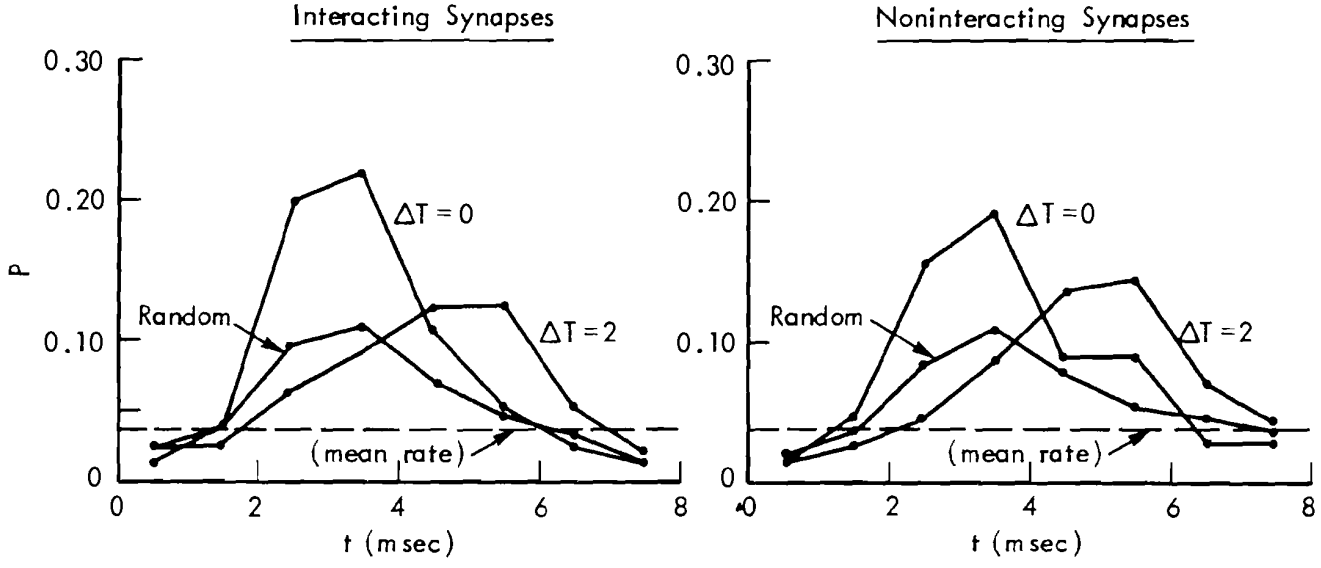

Fig. 6 -- Cross-correlation probability curves for threshold = 10 mv.

for $\Delta T = 0$ and $\Delta T = 2$ is larger in the interacting case than in the noninteracting case. In order to quantify these conclusions, we have considered three measures based on the cross-correlation statistics: the peak values of each probability curve (that is, the maximum probability value associated with single 1-msec bins); the probability that an output spike occurs in the 3-msec interval centered at the peak value; and the probability that an output spike occurs anytime in the first 8 msec following the event (as illustrated in Fig. 6, the range 0-8 msec contains the domain of influence of the input events in our cases). Table 2a displays these measures for the cases shown in Fig. 6. Table 2b shows how the probabilities for the coupled-pair cases compare to those for the random case. The probabilities are larger for $\Delta T = 0$ than for $\Delta T = 2$ for all measures in these tables.

Table 2

TRANSFER PROBABILITIES FOR CONTROL THRESHOLD = 10 mv

a. Direct Probabilities

	Interacting Synapses			Noninteracting Synapses		
Measure	Random	$\Delta T = 2$	$\Delta T = 0$	Random	$\Delta T = 2$	$\Delta T = 0$
1 bin	.1102	.1236	.2178	.1076	.1437	.1897
3 bins	.2787	.2988	.5215	.2680	.3506	.4339
8 bins	.4494	.5259	.6705	.4606	.5661	.6437

b. Normalized Probabilities, $P' \equiv P/P_{random}$

	Interacting Synapses			Noninteracting Synapses		
Measure	Random	$\Delta T = 2$	$\Delta T = 0$	Random	$\Delta T = 2$	$\Delta T = 0$
1 bin	1.00	1.12	1.98	1.00	1.34	1.76
3 bins	1.00	1.07	1.87	1.00	1.31	1.62
8 bins	1.00	1.17	1.49	1.00	1.23	1.40

In Fig. 7 the data of Table 2 (along with those for $\Delta T = 1$ in this case) are plotted to illustrate the coincidence sensitivity of the model. Figure 7 also contains a corresponding curve based on pure summation of two individual PSPs. It is clear that the mechanisms of the model produce a more marked coincidence sensitivity than is suggested by the pure summation of PSPs. This is most noticable for the 1-msec bin measures and for the case of interacting synapses.

SIX VALUES OF CONTROL THRESHOLDS

The conclusions based on the case where the control threshold = 10 mv hold generally for all the cases considered here. Figure 8 shows the probability curves for all of our cases. Table 3a shows our three measures of these probabilities as well as the mean output firing rate, w_o, for all cases. Tables 3b and 3c show the same data normalized in two different ways. Figure 9 shows the coincidence sensitivity, as determined by the normalized data in these tables, for all the cases.

We can consider the probability values for our 1-bin and 3-bin measures as reflecting the probability of time-locking between input event and output spike; the values for our 8-bin measure (and, more crudely, the mean output rate), on the other hand, reflect the gross effectiveness of the input event in producing a spike anywhere in its domain of influence.

The conclusions implied by the results of Table 3 and Figs. 8 and 9, then, are clear. As regards the probability of an output spike being associated in time with the input event (1-bin and 3-bin measures): the $\Delta T = 0$ pairs are more effective than the $\Delta T = 2$ pairs in all cases; the difference between the $\Delta T = 0$ and $\Delta T = 2$ results are greater than suggested by pure summation in all cases; the difference between the $\Delta T = 0$ and $\Delta T = 2$ responses are greater when there is interaction between synapses than when there is not. As regards the gross effectiveness of the input event (8-bin measure and mean firing rate): the above conclusions apply as long as the threshold is sufficiently high;

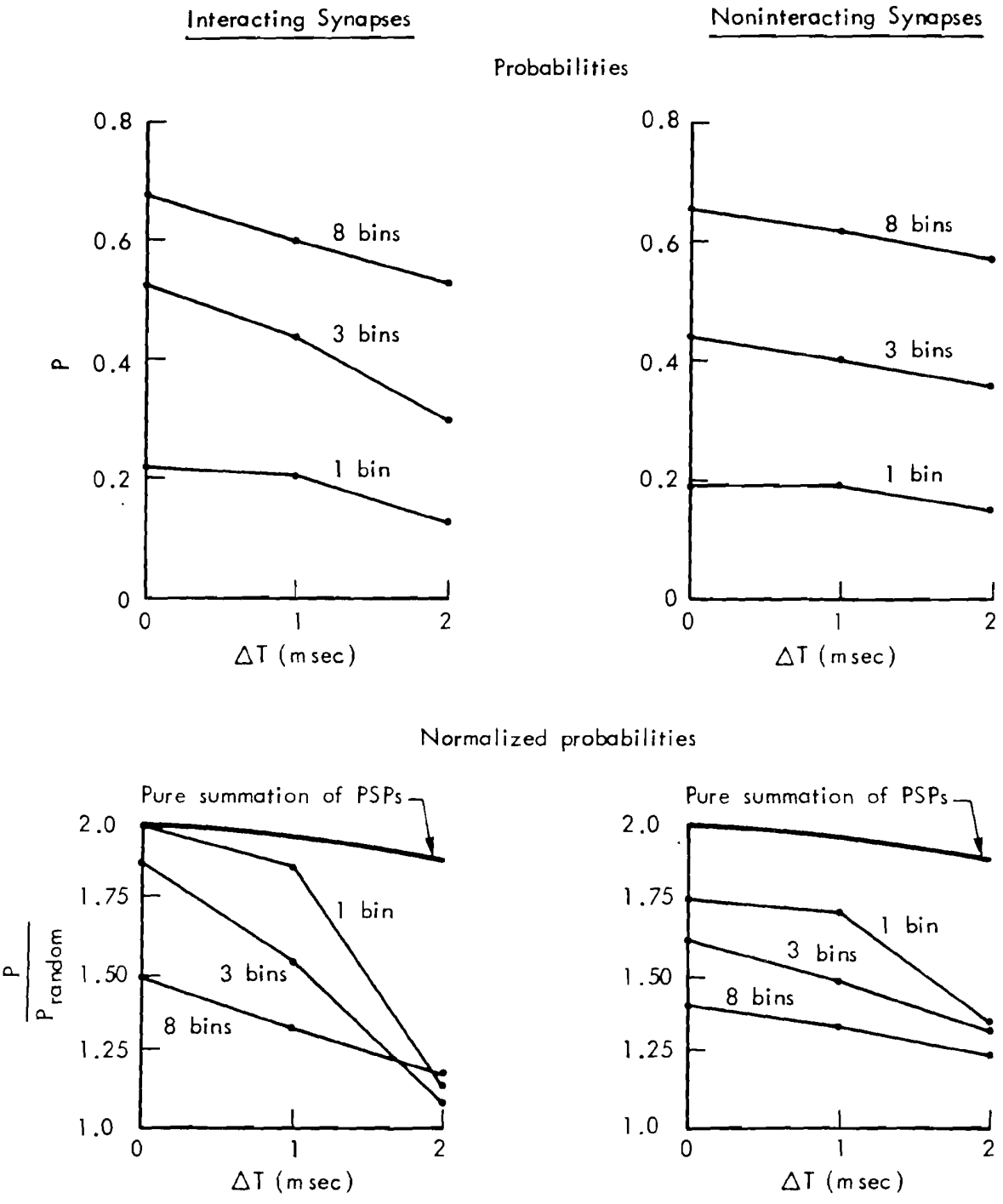

Fig. 7 -- Coincidence ~~sensitivity~~ curves for control threshold = 10 mv.

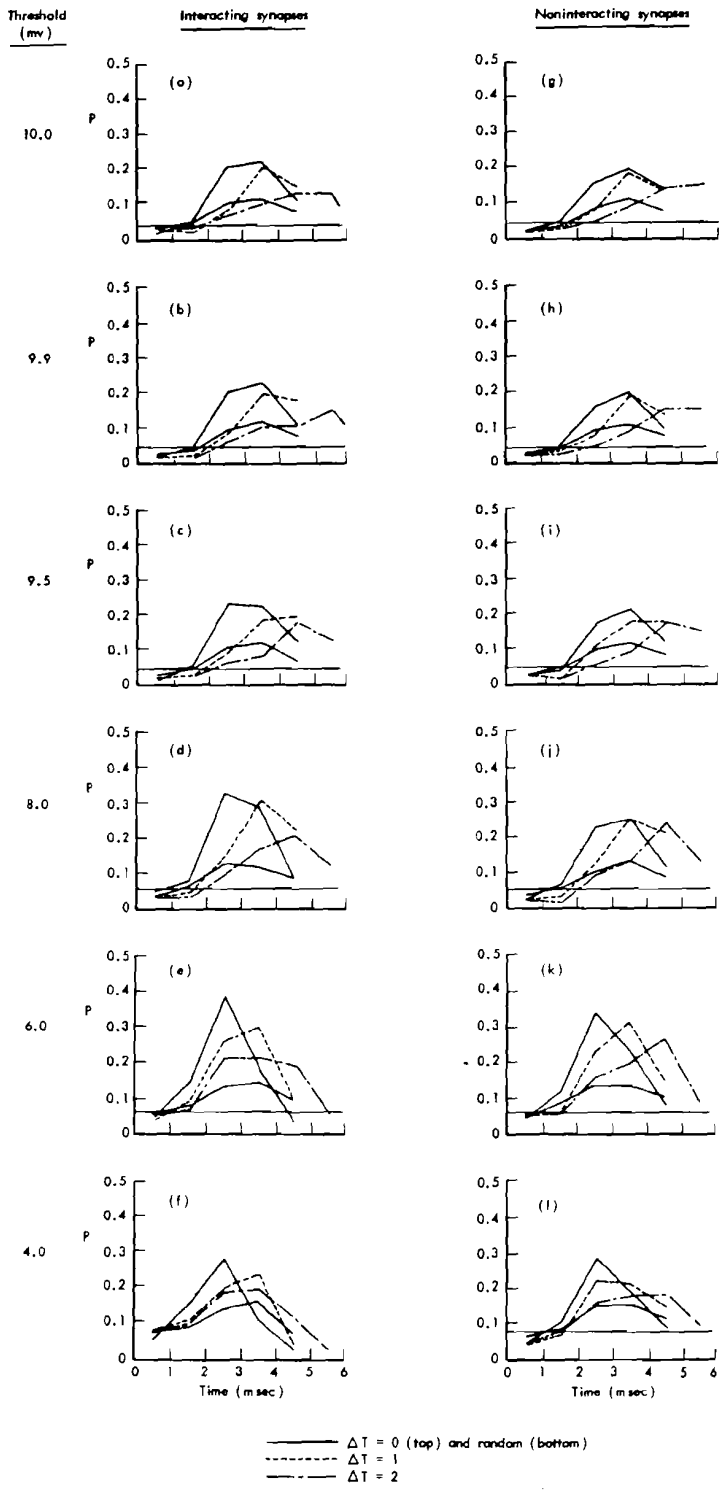

Fig. 8 -- Cross-correlation probability curves for six values of control threshold.

Table 3

TRANSFER PROBABILITIES FOR SIX VALUES OF CONTROL THRESHOLD

a. Direct Probabilities

Threshold	Measure	Interacting Synapses				Noninteracting Synapses			
		Random	ΔT = 2	ΔT = 1	ΔT = 0	Random	ΔT = 2	ΔT = 1	ΔT = 0
10.0	1 bin	.1102	.1236	.2063	.2178	.1076	.1437	.1839	.1897
	3 bins	.2787	.2988	.4327	.5215	.2680	.3506	.3966	.4339
	8 bins	.4494	.5259	.5960	.6705	.4606	.5661	.6121	.6437
	ω_0	38.3	38.3	41.9	43.8	38.9	39.9	41.9	43.8
9.9	1 bin	.1175	.1494	.1948	.2292	.1076	.1437	.1897	.1954
	3 bins	.2822	.3132	.4556	.5416	.2714	.3535	.4052	.4425
	8 bins	.4567	.5345	.6046	.6905	.4644	.5718	.6236	.6466
	ω_0	39.2	39.5	42.6	45.7	39.2	40.6	42.6	44.1
9.5	1 bin	.1192	.1782	.1948	.2321	.1119	.1724	.1753	.2069
	3 bins	.2946	.3937	.4327	.5100	.2882	.4080	.4483	.4914
	8 bins	.4841	.5718	.6504	.7278	.4953	.6006	.6609	.6724
	ω_0	41.7	42.5	45.9	48.7	42.0	42.7	45.0	46.6
8.0	1 bin	.1312	.2063	.3066	.3238	.1261	.2356	.2436	.2493
	3 bins	.3062	.4928	.6705	.6877	.3212	.4943	.5731	.5903
	8 bins	.5523	.6877	.8166	.8596	.5648	.7069	.7622	.7822
	ω_0	50.1	51.7	54.7	56.1	48.9	51.2	53.1	53.7
6.0	1 bin	.1463	.2092	.2951	.3811	.1341	.2665	.3152	.3324
	3 bins	.3648	.6046	.6562	.7106	.3494	.5502	.6877	.6877
	8 bins	.6266	.7994	.7937	.7937	.6587	.8481	.8510	.8395
	ω_0	61.2	58.9	59.6	59.8	60.9	59.6	69.6	59.2
4.0	1 bin	.1460	.1920	.2321	.2808	.1545	.1805	.2235	.2865
	3 bins	.3874	.4843	.4757	.5387	.4204	.4556	.5072	.5788
	8 bins	.6730	.7708	.7364	.6938	.7590	.8109	.8052	.7994
	ω_0	72.2	69.8	68.8	70.0	78.2	76.8	76.8	76.4

Table 3 -- continued

TRANSFER PROBABILITIES FOR SIX VALUES OF CONTROL THRESHOLD

b. Normalized Probabilities, $P' \equiv \frac{P}{P_{random}}$

Threshold	Measure	Interacting Synapses				Noninteracting Synapses			
		Random	ΔT = 2	ΔT = 1	ΔT = 0	Random	ΔT = 2	ΔT = 1	ΔT = 0
10.0	1 bin	1.0	1.122	1.872	1.976	1.0	1.336	1.709	1.763
	3 bins	1.0	1.072	1.553	1.871	1.0	1.308	1.480	1.619
	8 bins	1.0	1.170	1.326	1.492	1.0	1.229	1.329	1.398
	ω_0	1.0	1.00	1.09	1.17	1.0	1.03	1.08	1.13
9.9	1 bin	1.0	1.271	1.658	1.951	1.0	1.336	1.763	1.816
	3 bins	1.0	1.110	1.614	1.919	1.0	1.303	1.493	1.630
	8 bins	1.0	1.170	1.324	1.512	1.0	1.231	1.343	1.392
	ω_0	1.0	1.01	1.09	1.17	1.0	1.04	1.09	1.13
9.5	1 bin	1.0	1.495	1.634	1.947	1.0	1.541	1.567	1.849
	3 bins	1.0	1.336	1.469	1.731	1.0	1.416	1.556	1.705
	8 bins	1.0	1.181	1.344	1.503	1.0	1.213	1.334	1.358
	ω_0	1.0	1.02	1.10	1.17	1.0	1.02	1.07	1.11
8.0	1 bin	1.0	1.572	2.337	2.468	1.0	1.868	1.932	1.977
	3 bins	1.0	1.609	2.190	2.246	1.0	1.539	1.784	1.838
	8 bins	1.0	1.245	1.479	1.556	1.0	1.252	1.350	1.385
	ω_0	1.0	1.03	1.09	1.12	1.0	1.05	1.09	1.10
6.0	1 bin	1.0	1.430	2.017	2.605	1.0	1.987	1.667	2.478
	3 bins	1.0	1.657	1.799	1.948	1.0	1.575	1.968	1.968
	8 bins	1.0	1.276	1.267	1.267	1.0	1.288	1.292	1.274
	ω_0	1.0	.962	.974	.977	1.0	.979	.979	.972
4.0	1 bin	1.0	1.315	1.590	1.923	1.0	1.168	1.447	1.854
	3 bins	1.0	1.250	1.228	1.391	1.0	1.084	1.206	1.377
	8 bins	1.0	1.145	1.094	1.031	1.0	1.068	1.061	1.053
	ω_0	1.0	.967	.953	.970	1.0	.982	.982	.977

Table 3 -- continued

TRANSFER PROBABILITIES FOR SIX VALUES OF CONTROL THRESHOLD

c. Normalized Probabilities, $P'' \equiv \frac{P - (\text{Mean Rate})}{P_{random} - (\text{Mean Rate})}$

Threshold	Measure	Interacting Synapses				Noninteracting Synapses			
		Random	ΔT = 2	ΔT = 1	ΔT = 0	Random	ΔT = 2	ΔT = 1	ΔT = 0
10.0	1 bin	1.0	1.19	2.34	2.50	1.0	1.53	2.11	2.20
	3 bins	1.0	1.12	1.94	2.48	1.0	1.55	1.85	2.10
	8 bins	1.0	1.54	2.03	2.55	1.0	1.71	2.01	2.23
	ω_0								
9.9	1 bin	1.0	1.406	1.987	2.427	1.0	1.528	2.200	2.284
	3 bins	1.0	1.188	2.053	2.576	1.0	1.534	1.870	2.112
	8 bins	1.0	1.544	2.034	2.634	1.0	1.712	2.056	2.208
	ω_0								
9.5	1 bin	1.0	1.761	1.975	2.457	1.0	1.866	1.907	2.359
	3 bins	1.0	1.585	1.815	2.271	1.0	1.739	1.987	2.253
	8 bins	1.0	1.583	2.105	2.619	1.0	1.661	2.040	2.112
	ω_0								
8.0	1 bin	1.0	1.926	3.163	3.375	1.0	2.418	2.522	2.596
	3 bins	1.0	2.197	3.337	3.447	1.0	1.992	2.444	2.542
	8 bins	1.0	1.984	2.745	3.028	1.0	1.819	2.137	2.252
	ω_0								
6.0	1 bin	1.0	1.739	2.749	3.759	1.0	2.809	3.474	3.709
	3 bins	1.0	2.323	2.608	2.908	1.0	2.205	3.029	3.029
	8 bins	1.0	2.261	2.220	2.220	1.0	2.104	2.121	2.054
	ω_0								
4.0	1 bin	1.0	1.623	2.167	2.827	1.0	1.341	1.904	2.730
	3 bins	1.0	1.567	1.517	1.886	1.0	1.189	1.967	1.853
	8 bins	1.0	2.025	1.664	1.218	1.0	1.389	1.346	1.303
	ω_0								

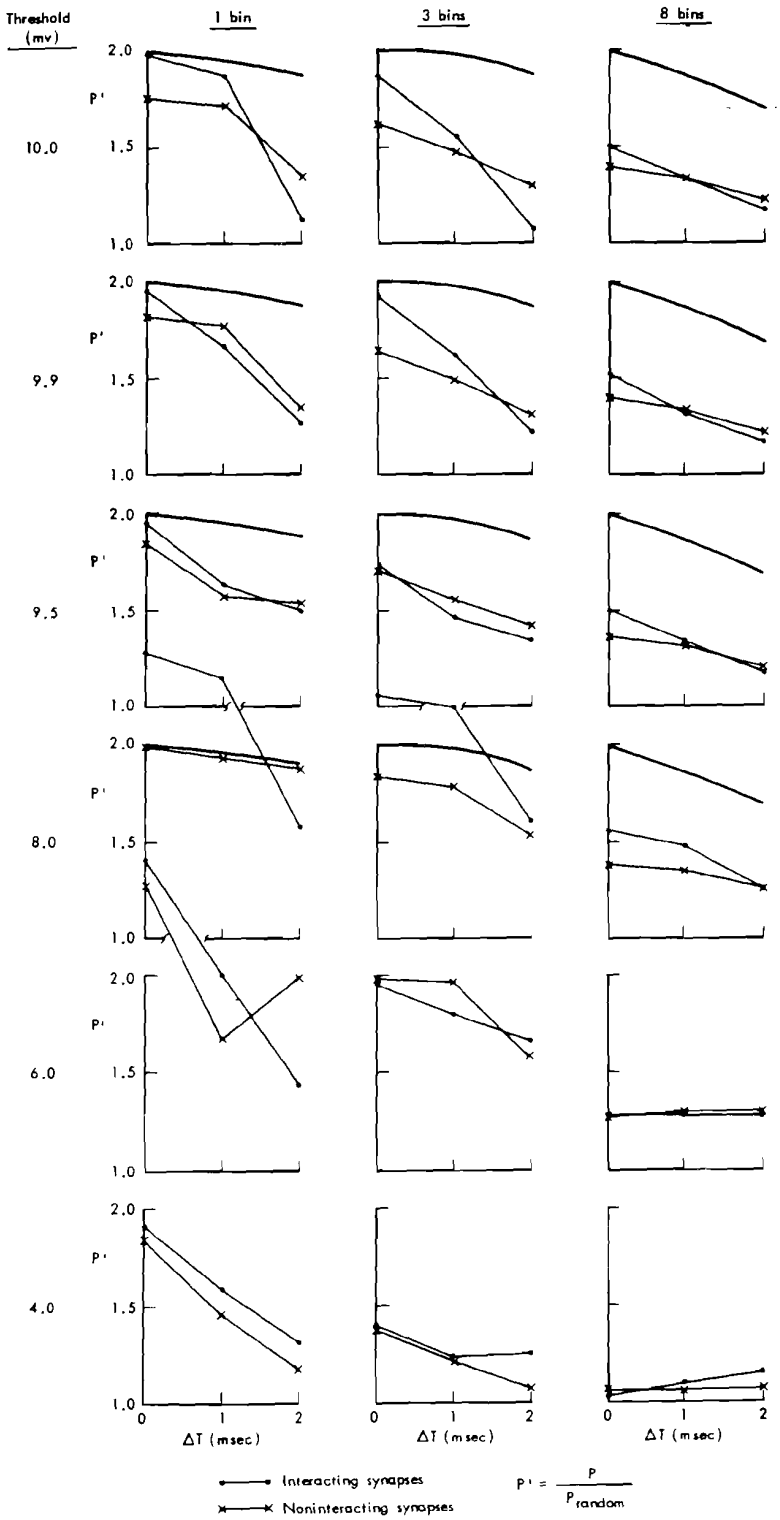

Fig. 9a -- Normalized coincidence sensitivity for six values of control threshold.

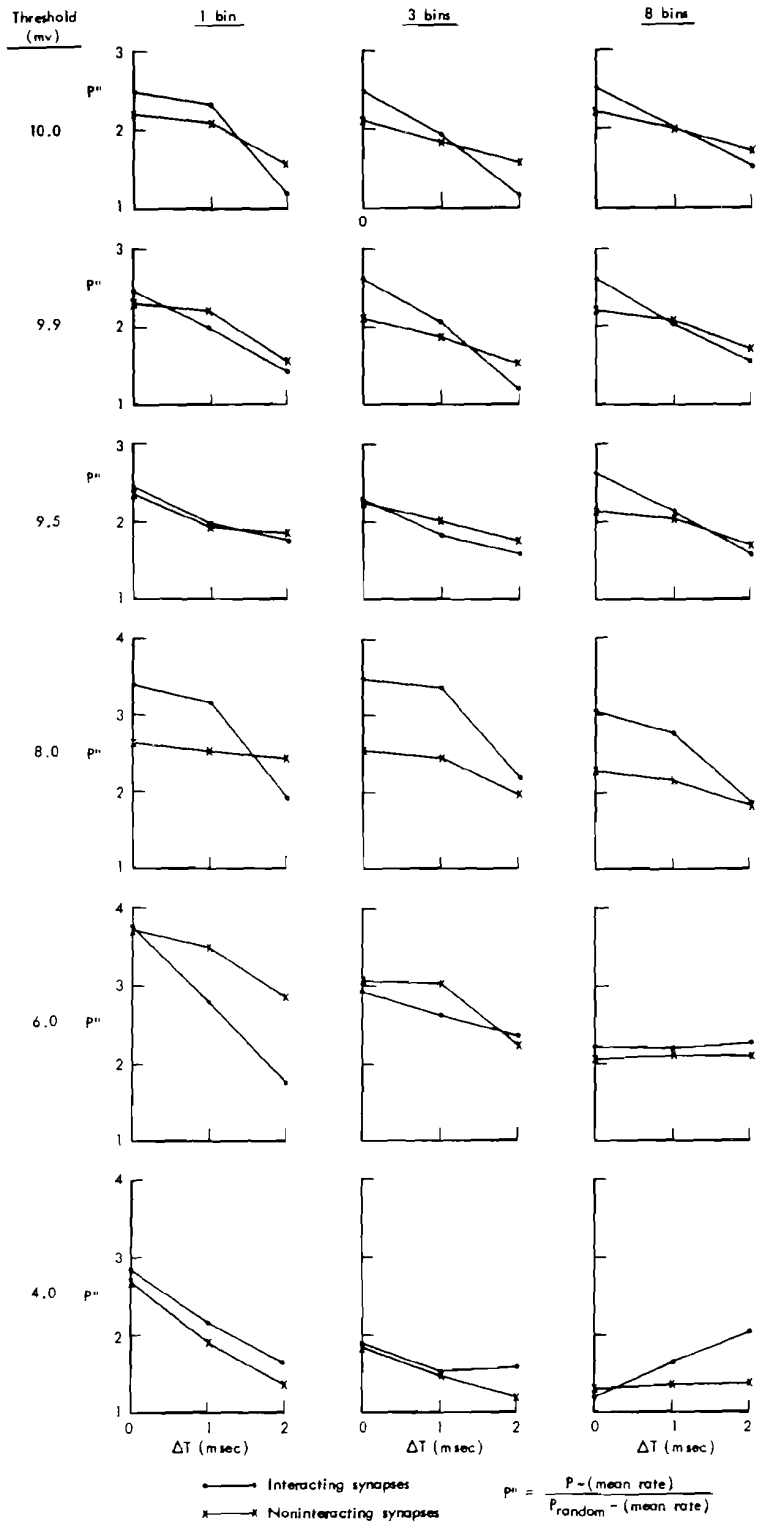

Fig. 9b -- Normalized coincidence sensitivity for six values of control threshold.

when the threshold decreases to 6 and to 4 mv in our cases, the probability values for $\Delta T = 2$ are sometimes higher than for $\Delta T = 0$, suggesting that distinctions between the two cases ($\Delta T = 0$ versus $\Delta T = 2$) based on their gross effectiveness are masked by the background activity at these output firing rates. (It is important to emphasize, however, that the probabilities for time-locking are not so masked.)

In the following section we consider more closely the influence of background activity as it relates to the ability of the cell to discriminate between the $\Delta T = 0$ and $\Delta T = 2$ cases.

INFLUENCE OF BACKGROUND ACTIVITY

In this section we present results of simulations that indicate the influence of background activity on coincidence discrimination, and then the data from the cases described above in this context.

In the following simulations we have used the same input patterns used in the foregoing sections for the cases $\Delta T = 0$ and $\Delta T = 2$. Figure 10 shows the dendritic tree simulated in this section. This situation, then, presents a series of coupled pairs of input pulses in two interacting synapses 0.1 length constant apart, together with random background activity (frequency = 275 pulses per second) from an independent source. (The synaptic currents of the background activity do not interact with each other or with those of the coupled pulses.) We have varied in these simulations the amplitude of the PSPs in the background train. Values of 5, 14, 23, 32, 41, and 50 mv (evaluated at the synapses) have been used. The control amplitude of the PSPs in the interacting synapses was 25 mv (evaluated at the synapses) for all six of these cases.

Table 4 shows the transfer probabilities for these cases. The top four plots in Fig. 11 show how the probabilities vary with background pulse amplitude, while the bottom two show how the difference in probability between the cases for $\Delta T = 0$ and $\Delta T = 2$ varies with background pulse amplitude. Figure 11 shows that the difference between the coincident and $\Delta T = 2$ cases (i.e., what we here call "coincidence sensitivity") exhibits a maximum value at an intermediate value of background pulse amplitude, as do the actual values of the peak probabilities.

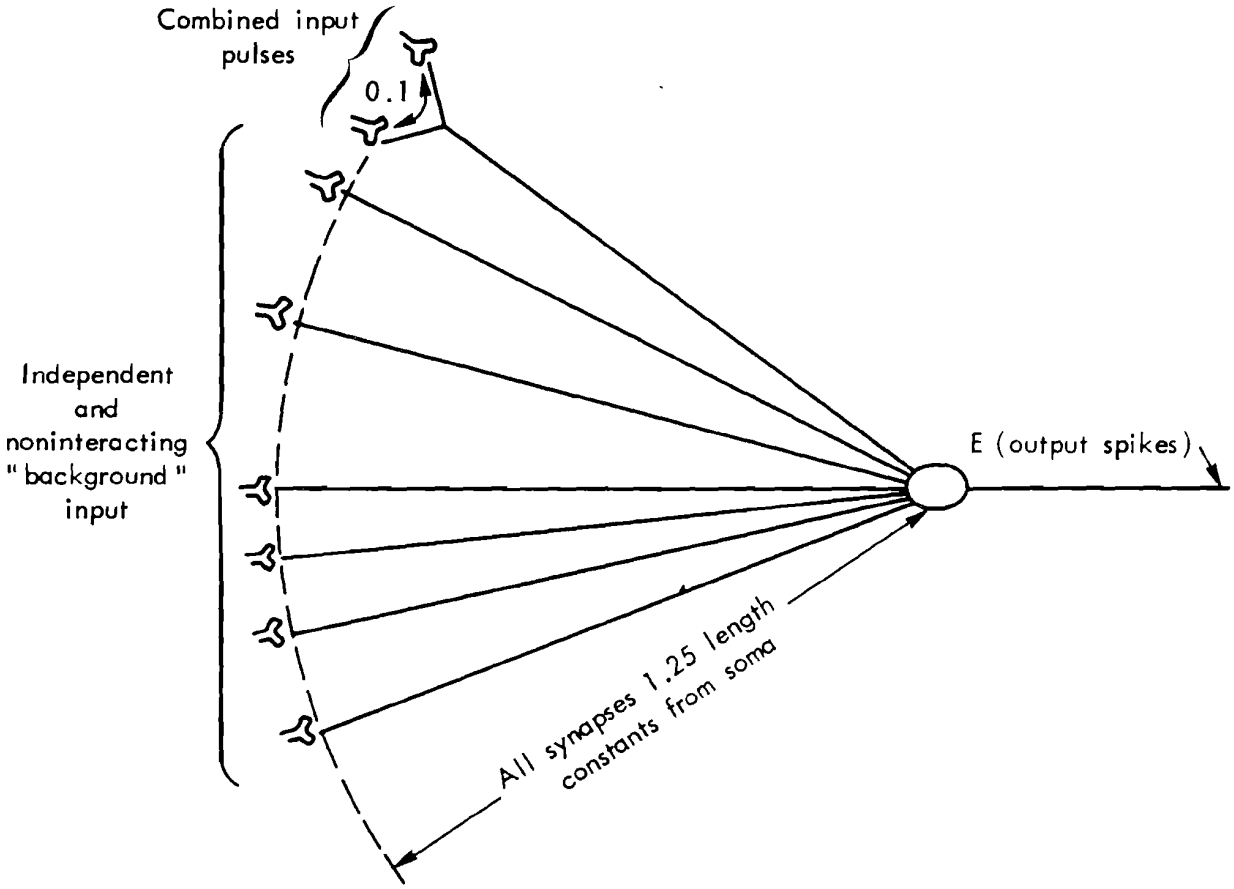

Fig. 10 -- Dendritic tree simulated in the investigation of the influence of background activity on coincidence sensitivity.

Table 4

TRANSFER PROBABILITIES VERSUS BACKGROUND PULSE AMPLITUDE

	$\omega_{background}$ = 274.1				$\omega_{background}$ = 548.2			
Measure	A	$\Delta T = 0$	$\Delta T = 2$	$\Delta T_0 - \Delta T_2$	A	$\Delta T = 0$	$\Delta T = 2$	$\Delta T_0 - \Delta T_2$
1 bin	1.52	.1035	.1006	.0029	0.76	.1412	.1134	.0278
3 bins		.2069	.1494	.0575		.2017	.1337	.0680
8 bins		.2069	.1494	.0575		.2017	.1337	.0680
ω_0		12.1	8.72	...		11.8	7.8	...
1 bin	4.25	.2730	.1868	.0862	2.13	.3209	.2213	.0996
3 bins		.5604	.4052	.1552		.5989	.4224	.1765
8 bins		.6695	.5172	.1523		.6246	.4943	.1303
ω_0		39.9	32.2	...		36.1	28.8	...
1 bin	6.97	.3267	.2464	.0803	3.48	.5272	.4900	.0372
3 bins		.6820	.5301	.1519		.9742	.9169	.0573
8 bins		.8682	.7708	.0974		1.0000	.9914	.0086
ω_0		56.8	54.1	...		58.5	58.5	...
1 bin	9.89	.2292	.1691	.0601	4.95	.3725	.3095	.0630
3 bins		.4757	.4183	.0574		.6676	.6275	.0401
8 bins		.7536	.7622	-.0086		.8510	.8997	-.0487
ω_0		74.8	73.3	...		69.6	69.3	...
1 bin	12.5	.2280	.1839	.0441	6.25	.1745	.1433	.0312
3 bins		.4788	.4419	.0369		.4564	.3800	.0764
8 bins		.8730	.8710	.0020		.8691	.8900	-.0209
ω_0		94.8	94.1	...		97.7	97.1	...
1 bin	15.2	.2333	.2344	-.0011	7.60	.2349	.1910	.0439
3 bins		.5889	.5641	.0248		.5000	.4832	.0168
8 bins		.9704	.9597	.0107		.9697	.9700	-.0003
ω_0		107.9	106.7	...		110.1	108.9	...

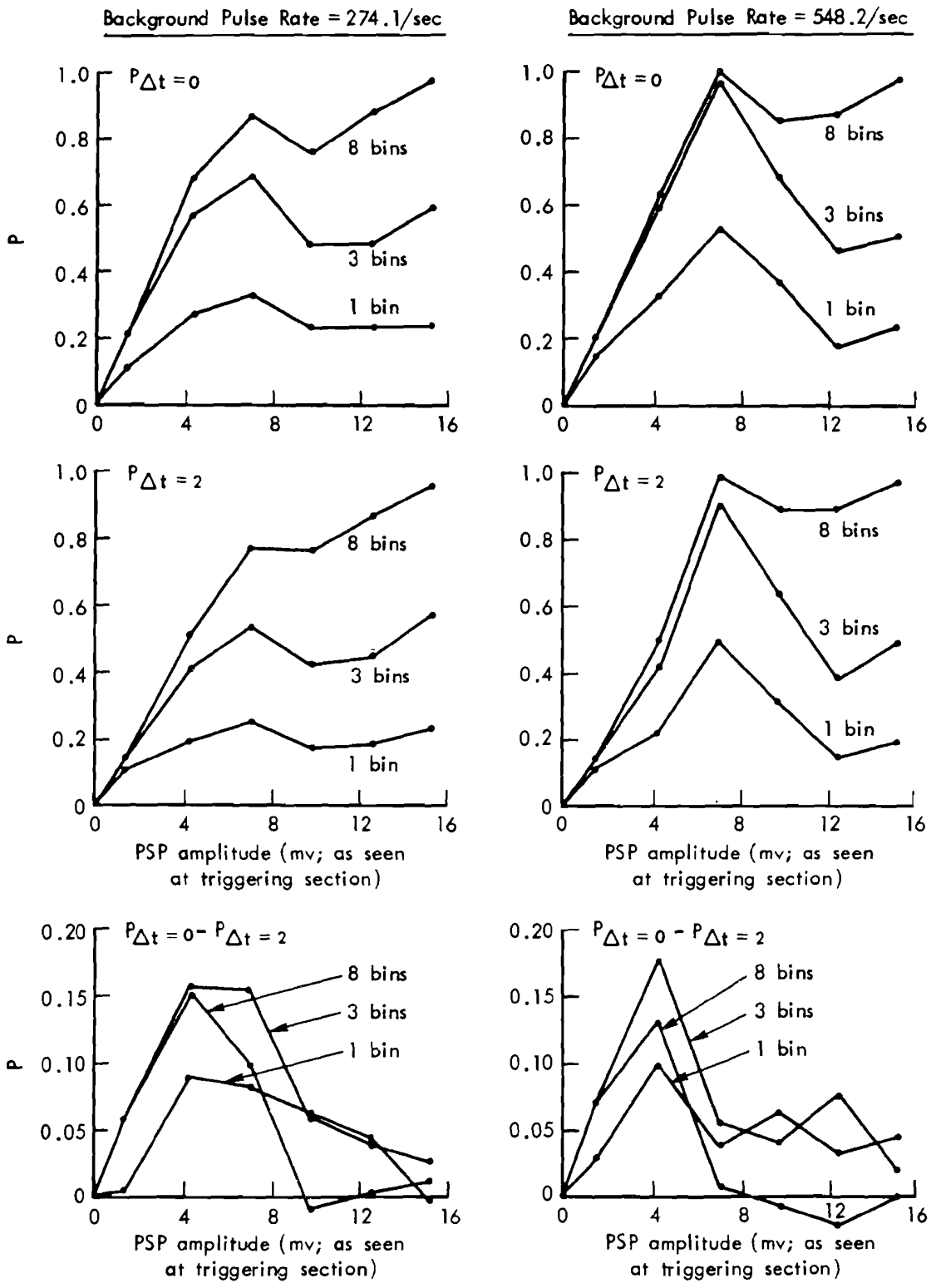

Fig. 11 -- Cross-correlation probability values as influenced by the amplitude of background pulses.

The difference curves based on time-locking of input to output (1 bin and 3 bins) exhibit positive values over an extremely wide range of background pulse amplitude. This shows that the coincident input event is more likely to localize an output spike in time than is the $\Delta T = 2$ input event throughout this range. The difference between these input patterns as regards their general effectiveness in contributing to an output spike (8 bins), however, disappears at high values of background pulse amplitude.

Figure 12 shows the probability values from our previous simulations (Table 3a) as a function of the control threshold values used there. Since one may suppose that decreasing the control threshold value has the same effect as adding a completely flat excitation to the cell from an independent source, these curves give an indication of how the difference between the probabilities for $\Delta T = 0$ and $\Delta T = 2$ should be influenced by a very flat extraneous source of excitation.

As may be seen in Fig. 12, the probabilities exhibit a maximum value at some intermediate threshold value for all the input cases involving coupled pairs of pulses. These curves exhibit the same general trends as those discussed above for Fig. 11.

INFLUENCE OF SPATIAL SEPARATION OF INTERACTING SYNAPSES

As discussed in Section IV, the interaction of synaptic currents between neighboring synapses is one of the reasons why our results show a higher coincidence sensitivity than one obtains by pure addition of PSPs. Since the smaller the distance between two synapses, the more their synaptic currents can interact, it follows that the smaller the distance between two synapses, the better they will discriminate small intervals of time between pulses activating them. That is, the differences in responses for $\Delta T = 0$ and $\Delta T = 2$, say, should be greater, the closer the two interacting synapses. We have performed a set of simulations to illustrate this point. In the simulations described in the first part of the Results section, we placed interacting synapses at locations I and III in the dendritic tree shown in Fig. 2. Those

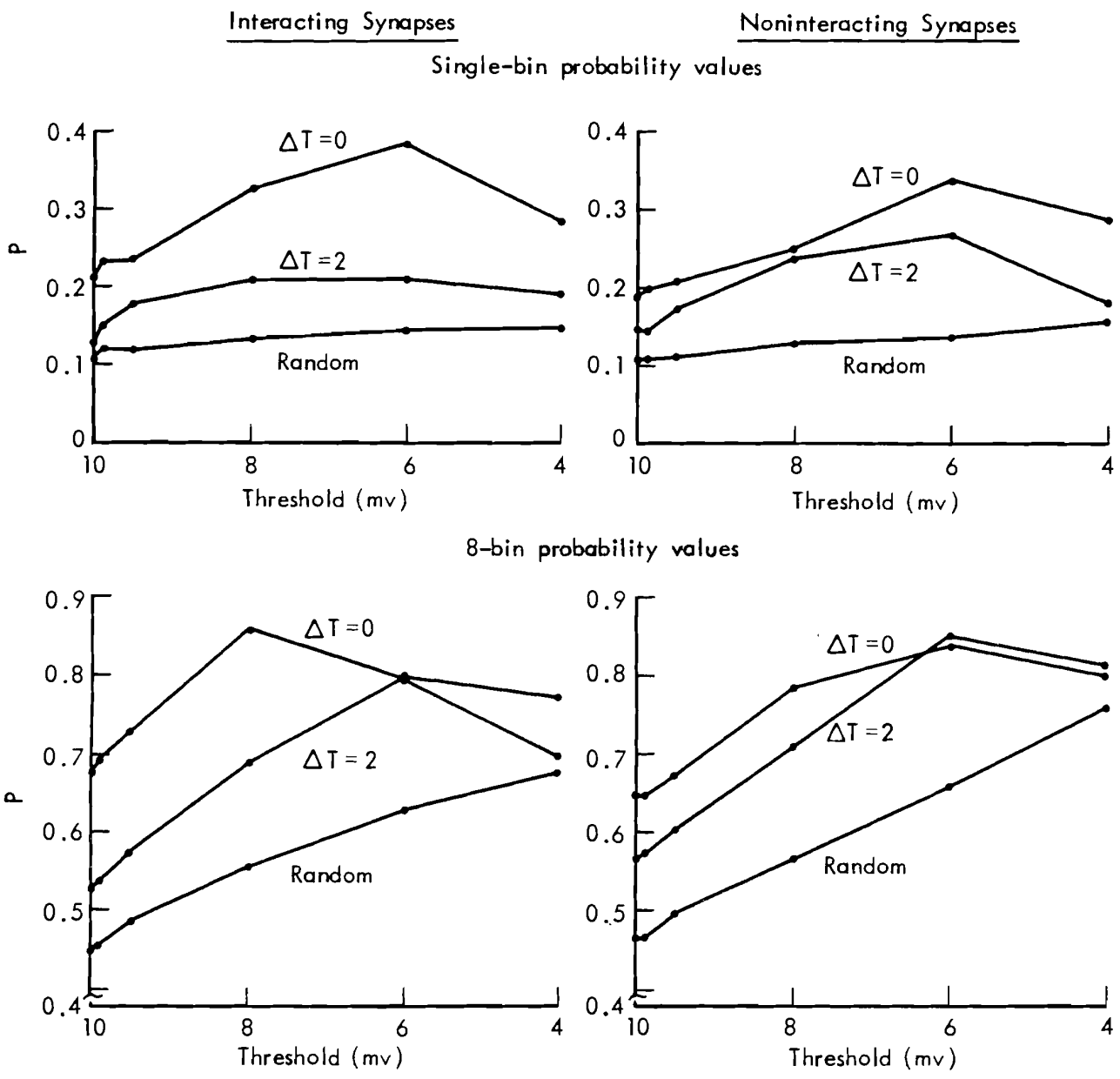

Fig. 12 -- Cross-correlation probability values as influenced by the control threshold value.

synapses were 0.25 length constant apart. For the present simulations, we used precisely the same temporal structure for our input, but placed the interacting synapses at I and II. (The input parameters shown in Table 1 were interchanged for synapses II and III.) In this case, then, the interacting synapses are 0.1 length constant apart. We examined the random, $\Delta T = 0$, 1, and 2 input patterns, used control PSPs of 25 mv, and used a control threshold of 10 mv.

Table 5 shows the transfer probabilities for these cases.

Table 5

TRANSFER PROBABILITIES VERSUS AMOUNT OF SYNAPTIC INTERACTION

Case	Measure	Probability Values (P)				Normalized Values (P/P_{random})			
		Random	$\Delta T = 2$	$\Delta T = 1$	$\Delta T = 0$	Random	$\Delta T = 2$	$\Delta T = 1$	$\Delta T = 0$
$\Delta x = .1$	1 bin	.1111	.1236	.1638	.2321	1.0	1.1125	1.4743	2.0891
	3 bins	.2796	.2845	.4167	.5444	1.0	1.0175	1.4903	1.9470
	8 bins	.4511	.5086	.5833	.6963	1.0	1.1274	1.2930	1.5435
	ω_0	38.5	38.0	41.0	46.1	1.0	.987	1.0649	1.1974
$\Delta x = .25$	1 bin	.1102	.1236	.2063	.2178	1.0	1.122	1.872	1.976
	3 bins	.2787	.2988	.4327	.5215	1.0	1.072	1.553	1.871
	8 bins	.4494	.5259	.5960	.6705	1.0	1.170	1.326	1.492
	ω_0	38.3	38.3	41.9	43.8	1.0	1.00	1.09	1.17
Non-interacting	1 bin	.1076	.1437	.1839	.1897	1.0	1.336	1.709	1.763
	3 bins	.2680	.3506	.3966	.4339	1.0	1.308	1.480	1.619
	8 bins	.4606	.5661	.6121	.6437	1.0	1.229	1.329	1.398
	ω_0	38.9	39.9	41.9	43.8	1.0	1.03	1.08	1.13

Table 5 also includes for comparison the corresponding transfer probabilities for the previous cases where the threshold was 10 mv; these have been reproduced from Table 3, and include the case where the interacting synapses are 0.25 length constant apart and the case where the synapses do not interact.

Inspection of Table 5 shows that for $\Delta T = 0$, the probability values for $\Delta x = .1$ are greater than those for $\Delta x = .25$, which are in turn greater than those for the noninteracting case. For $\Delta T = 2$, on the other hand, the values for $\Delta x = .1$ are less than those for $\Delta x = .25$, which are in turn less than those for the noninteracting case. These statements hold for all three of our probability measures (1 bin, 3 bins, and 8 bins). Thus the difference in probability values for $\Delta T = 0$ and $\Delta T = 2$ is greater for $\Delta x = .1$ than for $\Delta x = .25$, which in turn is greater than that for the noninteracting case.

These coincidence sensitivities, as measured by the normalized values shown in Table 5, are displayed in Fig. 13. Figure 13 also shows the coincidence sensitivity obtained by pure summation of PSPs.

Figure 13 shows clearly that the coincidence sensitivity exhibited in our results is most marked for smaller bin sizes and for large levels of synaptic interaction. That is, for synapses very close together in dendrites, two coincident input pulses are much more likely to produce an output spike locked in time with the input pulses than are two input pulses separated by a small time interval. The single-bin measures for the $\Delta x = .1$ case, for example, show that the peak probability for coincident pulses is nearly two times that for pulses separated by 2 msec, and considerably larger than that for two pulses separated by just 1 msec.

34
AM - 5598

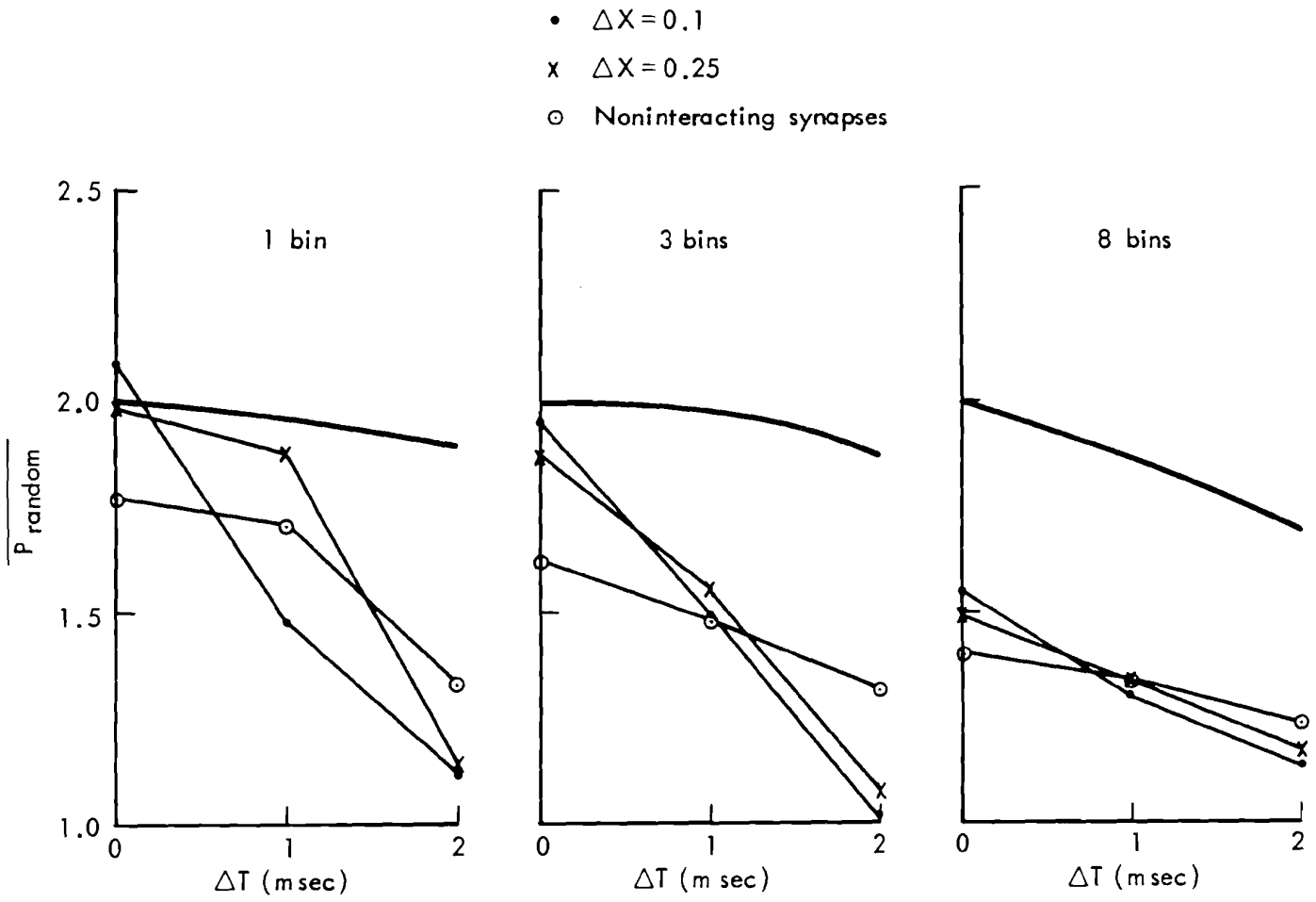

Fig. 13 -- Coincidence sensitivities for three levels of synaptic interaction.

IV. DISCUSSION AND CONCLUSIONS

The purpose of this Memorandum is to show that the "standard nerve cell" is indeed sensitive to the coincidence of input pulses in dendrites, despite the very flat character of the graded responses for these events, and more particularly that the cell is more likely to respond to two coincident pulses than to two pulses which are separated by a short time interval.

In this section we will first discuss the mechanisms which underlie this sensitivity, then provide a theoretical map to indicate how the continuum of possible background activity should influence the sensitivity, and finally, list our major conclusions.

Our concern with the question of coincidence sensitivity for dendritic synapses arose from the observation that PSPs which originate in dendrites often tend to be very flat as observed at the soma. We should note now that the time course of the PSP (as observed at the soma) differs markedly from the time course of the effectiveness of the pulse as regards the likelihood of initiating a spike. Figure 14a, for example, shows the time course of a single PSP as used in our model [Eq. (1) evaluated at $x - x^* = 1.25$] and cross-correlation probability curves for two of our random cases. The latter curves show as a function of time the probability that a single PSP with the shape shown in Fig. 14a will produce a spike for the conditions simulated in those cases. Figure 14 shows that the declining phase of the PSPs was very rarely associated with output spikes; that is, the PSPs tended to initiate spikes on their rising phases or not at all. Figure 14b shows that this observation applies as well to coupled pairs of PSPs.

The conclusion, then, is that the effectiveness of a PSP (or of a combination of PSPs) in terms of producing an output spike is considerably more localized in time than the PSP itself. The peak amplitude of the graded response is the important factor concerning its effectiveness.

Our computations illustrate that the relationship between peak amplitude and effectiveness as to output spike production is nonlinear. (The fact that our coincidence sensitivity curves for the noninteracting

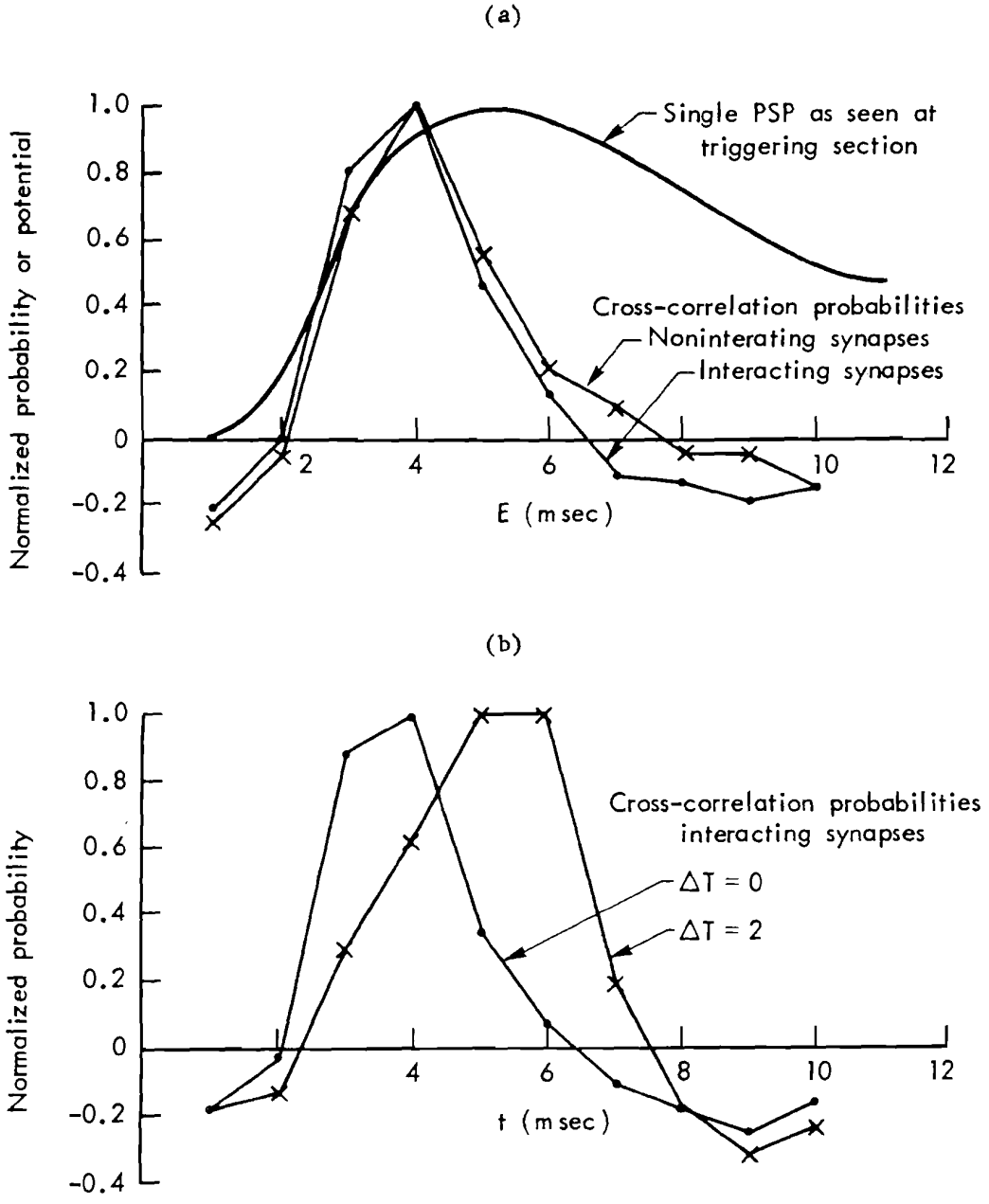

Fig. 14 -- Relative time courses of cross-correlation probabilities and of a single PSP. (Control threshold = 10 mv.)

case are generally sharper than those based on pure summation of PSPs, for example, illustrates this.) Moreover, the difference in peak amplitude in the graded responses (that is, the difference between the case involving coincident pulses and the case where the two input pulses are separated by a small interval of time) is amplified in the present model by the nonlinear interaction of synaptic currents. This interaction, therefore, further sharpens the coincidence sensitivity of the cell as compared to pure summation of PSPs. The essential factor in this mechanism is that the amplitudes of single PSPs are diminished according to the potential that exists across the subsynaptic membrane when the synapse is activated [Eq. (2)]. This implies that if one synapse is activated, say, 2 msec before a second nearby synapse is activated, then the PSP from the first synapse will occlude the PSP originating at the second synapse. The net response, as seen at the soma, will consist of the sum of one PSP with its particular control amplitude, together with a second PSP whose amplitude is less than its control value. Now, PSPs require a finite time to develop and propagate. Therefore, if the two synapses are activated simultaneously the interaction between them will be minimized. This is the mechanism which causes the present simulations to show a greater coincidence sensitivity for the case in which the synapses interact than for the case in which they do not.

Our present model cannot adequately indicate the extent to which this last-mentioned mechanism may operate in real nerve cells. The properties of the interaction of the synaptic currents will depend on the detailed time courses of the synaptic permeability changes, and our present model includes only the rough approximation to this interaction indicated in Eq. (2). We suspect that our simulations should be representative for cases involving large, very brief synaptic permeability changes. On the other hand, our result showing a sharper coincidence sensitivity for interacting synapses than for noninteracting synapses should be less applicable to cases involving long-lasting synaptic permeability changes. Indeed, a more detailed study of this point may reveal a dimension for identifying among nerve cells those which have specialized towards coincidence sensitivity by developing large and brief synaptic permeability changes.

Factors other than those considered in the present Memorandum may certainly be expected to contribute to coincidence sensitivity. Inhibitory synapses, for example, clearly could achieve this end. Another very relevant factor, relating to the Hodgkin-Huxley representation of excitable membrane,[8] suggests that coincidence sensitivity to excitatory PSPs should be greater than indicated by the present simulations:* in the present model we have represented a triggering section by a threshold rule which depends only on the value of the generator potential at a particular point in time and on the time interval since the last output spike. A more realistic representation of the triggering section would include the well-known fact that the Hodgkin-Huxley membrane is sensitive to the rate of rise of the generator potential: the cell is more easily excited by rapidly rising stimuli than by more gradually rising stimuli. Clearly, the generator potential for coincident pulses will exhibit a steeper rising phase (as well as a larger peak amplitude) than that for noncoincident pulses. One expects, then, that a more realistic representation of the triggering section of the nerve cell should heighten the coincidence sensitivity discussed here.

It is clear that the actual value of the probability that a given set of coincident pulses will initiate a spike depend on the quantity and character of the other input the cell is experiencing. It is not difficult, however, to provide a map to indicate generally how this influence operates. We can say that the probability that a given input event, E, will produce an output spike in the presence of other input activity, O, is an increasing function of [e + o - th(o)], where e and o are the amplitudes of the graded events associated with E and O, and th is the threshold. The threshold is an increasing function of o because of refractoriness; that is, increasing o increases the probability that the cell will have fired in a short time interval before E, and that E will therefore arrive during a refractory period. Any other input, O, then, which tends to produce output spikes will, on

---

*The author is grateful to John W. Moore for pointing out to him this implication for coincidence sensitivity in the Hodgkin-Huxley schema.

the one hand, facilitate the effectiveness of E by summation of graded responses, but on the other hand, will tend to decrease the effectiveness of E by increasing the likelihood that E encounters a refractory state. The facilitating effect should predominate for low values of o, whereas at high values of o the latter effect might be expected to predominate. The probability that E is associated with an output spike, then, should exhibit a maximum at an intermediate value of o for the case when the input constellation, O, is itself capable of generating output spikes. Also, one can convince himself that the difference in probability of output spike initiation for two cases E_1 and E_2, where $e_1 > e_2$, should also tend to exhibit a maximum value at an intermediate value of o in this case. (For very high o, e_2 will be just as likely as e_1 to be greater than th.) Both of these tendencies are seen in our Figs. 11 and 12.

Consider now the case where O is completely flat. Suppose that E is incapable of generating a spike by itself (that is, e < th). Clearly, the probability that E will produce a spike can be sketched as in Fig. 15.

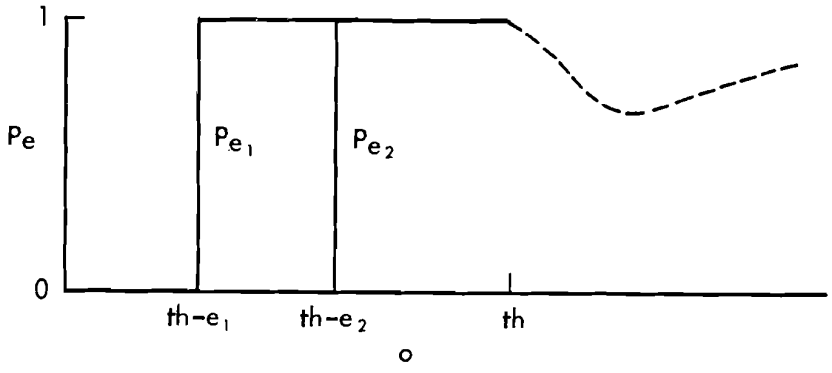

Fig. 15 -- Effectiveness of an input event as a function of the amplitude of smooth background activity.

That is, <u>any</u> input event E will be associated with an output spike with probability 1.0 for a certain range of smooth background activity. Also, for any two input events, E_1 and E_2, where $e_1 > e_2$, there will be a range of o where $p_1 = 1.0$ and $p_2 = 0$.

The purpose of the preceding paragraphs is to suggest the following points: the probability with which any given input event will be associated with an output spike may range from close to 0 to 1, depending on the input activity from other sources; the probability with which any given input event (which is itself incapable of producing a spike) will be associated with an output spike is influenced by the continuum of possible background activities as shown in qualitative terms in Fig. 16; the difference in effectiveness between two events E_1 and E_2, where $th > e_1 > e_2$, should exhibit a maximum at intermediate levels of background activity. As shown in Fig. 11, our results corroborate these conclusions.

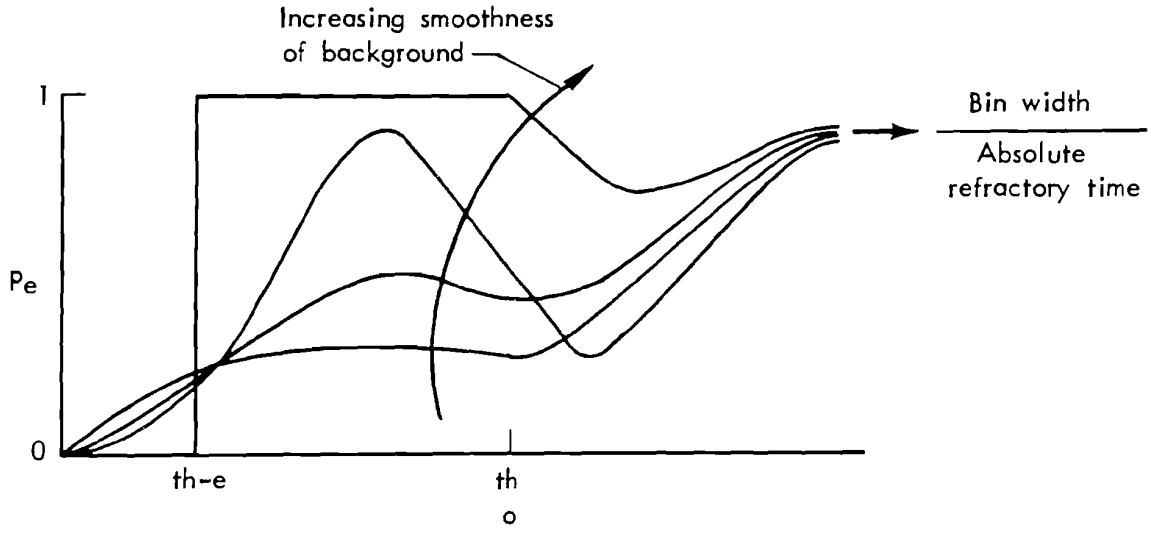

Fig. 16 -- Influence of character and magnitude of background activity on the effectiveness of a given input event.

Our simulation studies have shown, then, that for the present model

- the probability, p, that an output spike will be associated in time with a coupled pair of input pulses originating at dendritic synapses is greater when the time interval between the pulses is 0 than when it is 2 msec;
- both the actual values of the probabilities and their differences, $p(\Delta T = 0) - p(\Delta T = 2)$, are generally larger for smooth than for irregular background activity, and both the probabilities and their differences tend to display maxima at intermediate levels of background activity; and
- the difference $p(\Delta T = 0) - p(\Delta T = 2)$ is greater the closer together the two synapses.

It seems clear that our results show that the standard nerve cell should indeed exhibit sensitivity to the coincidence of input pulses originating in dendrites, in the sense that output events should be more likely to be associated with coincident than with temporally separated input events. This, then, is the answer provided by the simulations to our original question. The studies also pose the subsequent question: how are such probability differences utilized in the function of particular neural subsystems? It is not at all clear at this time, for example, what values of probability or probability differences may be regarded as "large". It is indeed an intriguing and important question; one which most likely will have many answers for the many and various subsystems one might consider, for the many functions each might be performing, and for the many conditions under which they might operate.

REFERENCES

1. Eccles, J. C., The Physiology of Nerve Cells, Johns Hopkins, Baltimore, 1957.

2. Rall, W., "Distinguishing Theoretical Synaptic Potentials Computed for Different Soma-Dendritic Distributions of Synaptic Input," J. Neurophysiol., Vol. 30, 1967, pp. 1138-1168.

3. MacGregor, R. J., "A Model for Responses to Activation by Axo-Dendritic Synapses," Biophys. J., Vol. 8, 1968, pp. 305-318.

4. -----, Input-output relations for axo-somatic activation in a neuron model, The Rand Corporation, Santa Monica, California, P-3672, 1967.

5. -----, A digital-computer model of spike elicitation by postsynaptic potentials in single nerve cells, The Rand Corporation, Santa Monica, California, RM-4877-ARPA, 1966.

6. Bullock, T. H., and C. A. Horridge, Structure and Function in the Nervous Systems of Invertebrates, Freeman Press, San Francisco, 1965.

7. Perkel, D. H., "Neuronal Spike Trains and Stochastic Point Process: I. The Single Spike Train;" "II. Simultaneous Spike Trains," Biophys. J., Vol. 7, 1967, pp. 391-418; pp 419-440.

8. Hodgkin, A. L., and A. F. Huxley, "A Quantitative Description of Membrane Current and Its Application to Conduction and Excitation in Nerve," J. Physiol., Vol. 117, 1952, pp. 500-544.